The Journal of Navigation (2024), 1–18
doi:10.1017/S0373463324000225

CAMBRIDGE UNIVERSITY PRESS

RESEARCH ARTICLE

Missed detection probability evaluation for the RAIM based on worst-case fault magnitude searching

Ruijie Li, Liang Li,* Liuqi Wang, Min Li, and Zhibo Na

School of Intelligent System Science and Engineering, Harbin Engineering University, Harbin, China.
*Corresponding author: Liang Li; Email: liliang@hrbeu.edu.cn

Received: 9 January 2023; **Revised:** 25 April 2024; **Accepted:** 11 June 2024

Keywords: RAIM; integrity; GNSS

Abstract

Missed detection probability is a critical metric for the integrity performance of receiver autonomous integrity monitoring (RAIM) in the presence of faults. The traditional missed detection probability evaluation method for RAIM is limited by impractical time consumption because of the absence of accurate searching interval for the magnitude of a worst-case fault. To address this issue, the searching interval for the magnitude of a worst-case fault is constructed by the combination of minimum detectable magnitude and minimum hazardous magnitude, and the searching interval adjustment is designed to avoid the absence of worst-case fault magnitude so that the maximum missed detection probability can be accurately evaluated. The simulation result indicates that the proposed method can achieve higher accuracy for the worst-case fault magnitude searching. Furthermore, the accuracy of worldwide evaluated missed detection rate can achieve an improvement of 57·66% at most by the proposed method for the different classical RAIM algorithms.

1. Introduction

Global navigation satellite system (GNSS)-based positioning is vulnerable to infrequent observation faults, such as satellite failures, which trigger potential integrity threats for the reliability of aircraft navigation. As a user terminal integrity monitoring approach, receiver autonomous integrity monitoring (RAIM) is consistently acknowledged as the ultimate safeguard for ensuring the integrity of satellite navigation services. RAIM is deployed to monitor and assess the impact of potential threats on satellite signals, contributing to the real-time reliability of aircraft navigation (Li et al., 2017). The classical RAIM algorithm is designed to satisfy the required navigation performance (RNP) of en route and the non-precision approach phase defined in civil aviation (Li et al., 2012). With the full deployment of a BeiDou navigation satellite system (BDS) and Galileo, an increased number of redundant observation signals becomes available. A renewed interest has been drawn to expand RAIM to satisfy the more demanding RNP, e.g. LPV-200 (Kaleta and Skorupski, 2019).

With this goal, many forms of RAIM algorithms have been developed to support worldwide LPV-200 service (Milner and Ochieng, 2011; Li et al., 2017). The probabilities of false alarm and missed detection must be evaluated to verify the performance of RAIM (Milner et al., 2020). False alarm events are the major source of continuity risk defined in the averaging sense, which is not the focus of this contribution. The probability of missed detection determines the integrity performance in the presence of a fault, which can be translated from the integrity risk of the RNP (Li et al., 2017). The hazardous events caused by the satellite failures can bring catastrophic consequences for the safety of satellite-based navigational applications. Therefore, it is crucial to utilise the missed detection probability evaluation (MDPE) for RAIM algorithms for safety of navigation services.

The MDPE is designed to evaluate the missed detection probability by artificially injecting an observation fault into the RAIM algorithm (Blanch and Walter, 2020). The observation fault should be specific with respect to the faulty satellite and the fault magnitude, which can also be called a fault mode. Correspondingly, the rigorous MDPE is defined as whether or not the maximum missed detection probability of the RAIM algorithm can be obtained by injecting the specific observation fault, because the maximum missed detection probability is conservatively assumed as the truth of the integrity capability of the RAIM algorithm. The faulty satellite can be obtained from exhaustive testing of all the available satellites. Currently, most studies focus on the determination of fault magnitude, which can be categorised into at least two groups.

The first group is the brute-forcing method. Theoretically, sufficient fault modes and sufficient collected samples can be simulated to carry out the evaluation with adequate precision. For example, Lee et al. (2021) analysed the sensitivity performance of advanced RAIM to the parameters of integrity support message by the brute-forcing simulation. Wang et al. (2023) verified the missed detection performance of the RAIM algorithm with different grades of integrity parameters based on the brute-forcing method. The advantage of the brute-forcing method is that *a priori* statistical distribution of the samples is not needed. However, the exhaustive testing of the fault mode is impractical for the time consumption due to the absence of the interval for the fault magnitude, particularly when there are different fault modes to be considered (Milner and Ochieng, 2009).

The second group is the MDPE based on the worst-case fault (WCF) magnitude. The WCF magnitude maximise the missed detection probability. Therefore, the concept of a WCF magnitude can be used to speed up the MDPE. For example, Joerger et al. (2014) used the WCF magnitude to compare the integrity performance of RAIM algorithms based on the fault detector of residual and solution separation, respectively. Blanch and Walter (2020) used the WCF magnitude searching method to estimate the maximum missed detection probability for the advanced RAIM stress testing. Zhu et al. (2023) tested the integrity performance of a multi-sensor navigation system against the WCF. Nevertheless, the searching interval of the WCF magnitude has not yet been clarified. An over-tight searching interval may exclude the WCF magnitude for a given fault mode, whilst an over-loose searching interval will introduce heavy computational burden and reduce the search efficiency. Ober (2003) and Milner and Ochieng (2011) introduced the concepts of minimum hazardous magnitude (*MHM*) and minimum detectable magnitude (*MDM*) to construct the searching interval of the WCF magnitude. Furthermore, Jiang and Wang (2014) proposed an optimised searching interval construction method to improve the WCF magnitude searching efficiency. However, the proposed searching interval construction is challenged by the absence of the WCF magnitude when the searching interval is over-tight. Therefore, the searching interval for the fault magnitudes must be clarified when confronting the demanding required performance requirement.

According to this analysis, the traditional MDPE methods for the RAIM integrity performance evaluation are restricted by the absence of accurate searching interval for the WCF magnitude. In order to achieve the rigorous MDPE, we must speed up the evaluation process by imposing an accurate searching interval for the WCF magnitude for a given fault mode. We construct the searching interval of the WCF magnitude by combination of the *MHM* and *MDM*. Furthermore, the searching interval adjustment strategy is designed to improve the searching accuracy of the WCF magnitude. Section 2 provides the simulation results and summarises the research findings.

2. Missed detection probability evaluation for RAIM

In this section, the MDPE method for RAIM is described, and the necessity of constructing the WCF magnitude searching interval is discussed. The probability of missed detection is the likelihood of the position error (PE) beyond the specified alarm limit (AL) or user-calculated protection level (PL), whilst the test statistic is less than the detection threshold. Without losing generality, the probability of missed detection can be expressed as (Zhai et al., 2020),

$$p_{\mathrm{md}} = P(|\varepsilon| > l \cap q < T|H_i) \tag{1}$$

https://doi.org/10.1017/S0373463324000225 Published online by Cambridge University Press

where $\varepsilon = \boldsymbol{h}^{*\mathrm{T}}(\boldsymbol{v} + \boldsymbol{f}_i)$ is least squares (LS) state estimate error, and $\boldsymbol{h}^* = \boldsymbol{\alpha}^{\mathrm{T}}(\boldsymbol{H}^{\mathrm{T}}\boldsymbol{H})^{-1}\boldsymbol{H}^{\mathrm{T}}$. Here, $\boldsymbol{\alpha}$ is the $m \times 1$ vector used to extract the interest state out of the full state vector. For example, using $\boldsymbol{\alpha} = \left[0\ 0\ 1\ \boldsymbol{0}_{(m-3)\times 1}^{\mathrm{T}}\right]^{\mathrm{T}}$ to extract the vertical PE (VPE). Since the VPE is more difficult to satisfy than the horizontal direction, we focus on the vertical performance in this contribution (Milner and Ochieng, 2011). $\boldsymbol{H}$ is the $n \times m$ normalised observation matrix; n denotes the number of elements of the state vector; m is the number of observations collected in an epoch; and $\boldsymbol{v}$ is the $n \times 1$ normalised observation noise vector composed of zero-mean, unit-variance independent and identically distributed random variables. The detailed calculation process of normalised observation matrix can be referred to (Joerger et al. (2014), where $\boldsymbol{f}_i$ is the $n \times 1$ fault vector, and H_i is the hypothesis of ith satellite fault (Angus, 2007). Note that we consider the single satellite fault in this contribution because it has been widely proven that the traditional RAIM algorithm is limited in capability to detecting only a single satellite fault. Furthermore, l represents AL or PL, depending on whether the AL of navigation operations is known or not; q represents the residual-based (RB) test statistic and is equal to the norm of the residual vector $\boldsymbol{r} = (\boldsymbol{I}_n - \boldsymbol{H}(\boldsymbol{H}^{\mathrm{T}}\boldsymbol{H})^{-1}\boldsymbol{H}^{\mathrm{T}})\boldsymbol{z}$, where $\boldsymbol{z}$ is the $n \times 1$ normalised observation vector. Note that we will denote the $(\boldsymbol{I}_n - \boldsymbol{H}(\boldsymbol{H}^{\mathrm{T}}\boldsymbol{H})^{-1}\boldsymbol{H}^{\mathrm{T}})$ as $\boldsymbol{M}$ in the following to simplify notation. If $\boldsymbol{f} = \boldsymbol{0}_{n\times 1}$, q follows a chi-squared distribution with n–m degrees of freedom. Otherwise, q follows a noncentral chi-squared distribution with n–m degrees of freedom and noncentrality parameter λ^2 (Zhao et al., 2020). The detection threshold T is obtained from the inverse chi-square distribution when the required false alarm probability under the fault-free hypothesis is given (Joerger et al., 2014).

Based on the LS estimator and the RB detector, the PE and the test statistic follow the normal distribution and the noncentral chi-square distribution, respectively. Furthermore, it has been proven that the PE and the constructed test statistic are independent of each other (Ober, 2003). Therefore, Equation (1) can be written as,

$$p_{\mathrm{md}} = p_{\mathrm{pf}} \times p_{\mathrm{nd}} = P\{|\varepsilon| > l|H_i\} \times P\{q < T|H_i\} \tag{2}$$

where p_{pf} is the probability of positioning failure; p_{nd} is the probability that test statistic is less than the detection threshold; and p_{pf} and p_{nd} can be expressed as (Blanch and Walter, 2020),

$$p_{\mathrm{pf}} = P\{|\varepsilon| > l|H_i\} = \Phi\left[\frac{l + \eta_i}{\sigma}\right] + \Phi\left[\frac{l - \eta_i}{\sigma}\right] \tag{3}$$

$$p_{\mathrm{nd}} = P\{q < T|H_i\} = \chi^2_{T,n-m}[\lambda_i^2] \tag{4}$$

where Φ is the tail cumulative distribution function (CDF) of a standard normal distribution; $\chi^2_{p1,p2}[\,\cdot\,]$ is the CDF of a noncentral chi-squared with the detection threshold $p1$ and degrees of freedom $p2$; and η_i and λ_i^2 correspond to the VPE and noncentrality parameter under the H_i hypothesis, respectively, and can be expressed as,

$$\begin{cases} \eta_i = \boldsymbol{h}^{*\mathrm{T}}\boldsymbol{f}_i = \boldsymbol{h}^{*\mathrm{T}}\boldsymbol{F}_i b \\ \lambda_i^2 = \boldsymbol{f}_i^{\mathrm{T}}\boldsymbol{M}\boldsymbol{f}_i = \boldsymbol{F}_i^{\mathrm{T}}\boldsymbol{M}\boldsymbol{F}_i b^2 \end{cases} \tag{5}$$

where $\boldsymbol{F}_i$ is $n \times 1$ vector to indicate the faulty satellite in fault vector $\boldsymbol{f}_i$. For example, $\boldsymbol{F}_1 = [1\ 0 \ldots\ 0]^T$ represents the failure that occurred on the first satellite, and b is the fault magnitude of satellite i and is the norm of fault vector $\boldsymbol{f}_i$.

Since the rigorous MDPE needs to obtain the maximum probability of missed detection given the WCF $\bar{\boldsymbol{f}}_i$,

$$\bar{p}_{md} = P(|\varepsilon| > l|H_i \cap \bar{\boldsymbol{f}}_i) \times P(q < T|H_i \cap \bar{\boldsymbol{f}}_i) \tag{6}$$

The maximum probability of missed detection can be accurately calculated when the WCF is provided. The posterior probability of missed detection $\bar{p}_{md}$ can be calculated by collecting the cases that the PE

https://doi.org/10.1017/S0373463324000225 Published online by Cambridge University Press

is larger than l whist the test statistic is less than the threshold. The calculated $\bar{p}_{md}$ is compared with the predefined P_{MD} to verify whether the missed detection probability of the RAIM is satisfied. Therefore, it is necessary to obtain the WCF for the rigorous MDPE.

The WCF is obtained when the WCF satellite is determined and the WCF magnitude is provided. It has been shown in Angus (2007) that the WCF satellite is the one that maximises the slope, which is defined as the ratio between the estimated PE and the noncentrality parameter. Therefore, the WCF satellite can be determined by comparing the slope of all potential faulty satellites. The determination process of WCF satellite can be expressed as,

$$\overline{\boldsymbol{F}} = \underset{\boldsymbol{F}_i}{\operatorname{argmax}}\, Slope_i = \underset{\boldsymbol{F}_i}{\operatorname{argmax}}\, \frac{\eta_i^{\mathrm{T}}\eta_i}{\lambda_i^2} = \underset{\boldsymbol{F}_i}{\operatorname{argmax}}\, \frac{\boldsymbol{F}_i^{\mathrm{T}}\boldsymbol{h}^{*}\boldsymbol{h}^{*\mathrm{T}}\boldsymbol{F}_i}{\boldsymbol{F}_i^{\mathrm{T}}\boldsymbol{M}\boldsymbol{F}_i} \tag{7}$$

The corresponding WCF magnitude $\bar{b}$ can be obtained by searching the fault magnitudes through a 1D search process,

$$\bar{b} = \underset{b}{\operatorname{argmax}} \left(\Phi\left[\frac{l + \boldsymbol{h}^{*\mathrm{T}}\overline{\boldsymbol{F}}b}{\sigma}\right] + \Phi\left[\frac{l - \boldsymbol{h}^{*\mathrm{T}}\overline{\boldsymbol{F}}b}{\sigma}\right] \right) \chi^2_{T,n-m}[\overline{\boldsymbol{F}}^{\mathrm{T}}\boldsymbol{M}\overline{\boldsymbol{F}}b^2] \tag{8}$$

where $\sigma = \sqrt{\boldsymbol{\alpha}^{\mathrm{T}}(\boldsymbol{H}^{\mathrm{T}}\boldsymbol{H})^{-1}\boldsymbol{\alpha}}$ is the standard deviation of the estimated state error. It is necessary to obtain the WCF magnitude to ensure the rigorousness of MDPE. However, the search for the WCF magnitude can introduce the impractical time consumption of the MDPE. Section 3 discusses the construction of the searching interval for the WCF magnitude to implement the MDPE.

3. Searching interval of the WCF magnitude

This section describes a method to establish the searching interval for the WCF magnitude, and the searching interval adjustment is designed to avoid the absence of WCF magnitude so that the maximum missed detection probability can be accurately evaluated.

3.1. Searching interval construction

The concepts of *MDM* and *MHM* can be used for the construction of a searching interval of the WCF magnitude (Jiang and Wang, 2014). *MDM* is the minimum fault magnitude to protect against the observation fault given the probability p_{nd}, and *MHM* is the minimum fault magnitude resulting in positioning failure provided the probability p_{pf} (Ober, 2003; Milner and Ochieng, 2011). They can be written as,

$$MDM = \frac{\lambda_{\mathrm{md,exp}}}{||\boldsymbol{M}\bar{\boldsymbol{F}}||} \text{ s.t. } p_{\mathrm{nd}} = p_{\mathrm{md,exp}} \tag{9}$$

$$MHM = \frac{l - K_{\mathrm{md,exp}}\sigma}{|\boldsymbol{h}^{*\mathrm{T}}\bar{\boldsymbol{F}}|} \text{ s.t. } p_{\mathrm{pf}} = p_{\mathrm{md,exp}} \tag{10}$$

where $p_{\mathrm{md,exp}}$ is the expected missed detection probability to construct the searching interval, and $p_{\mathrm{md,exp}}$ is usually set up as equal to the preset requirement P_{MD} (Milner and Ochieng, 2011). $\lambda_{\mathrm{md,exp}}$ is the non-centrality parameter determined by the expected missed detection probability. $K_{\mathrm{md,exp}}$ is defined as the quantile of the $p_{\mathrm{md,exp}}$ based on tail cumulative distribution function of a normal distribution,

$$K_{\mathrm{md,exp}} = \Phi^{-1}(p_{\mathrm{md,exp}}/2) \tag{11}$$

With the defined *MDM* and *MHM*, the searching interval of the WCF magnitude, which is denoted as $\mathscr{B}$, can be divided into three cases:

https://doi.org/10.1017/S0373463324000225 Published online by Cambridge University Press

Case 1: $MDM \leq MHM$, the missed detection probability based on Equation (2) for any fault magnitude is smaller than $p_{\mathrm{md,exp}}$, as demonstrated in Appendix A. Therefore, the WCF magnitude cannot be obtained given the $p_{\mathrm{md,exp}}$.

Case 2: $MHM < MDM$ and the candidate searching interval $\mathscr{B} \in (0, MHM) \cup (MDM, \infty)$, the missed detection probability for the fault magnitude from the candidate searching interval $\mathscr{B}$ is smaller than $p_{\mathrm{md,exp}}$. The proof can be found at Appendix B. Therefore, the WCF magnitude cannot be obtained for the candidate searching interval $\mathscr{B}$ in this case.

Case 3: $MHM < MDM$, when the candidate searching interval $\mathscr{B} \in [MHM, MDM]$, the calculated probability of missed detection for the magnitude from the candidate searching interval $\mathscr{B}$ can be either larger or smaller than $p_{\mathrm{md,exp}}$.

The searching interval should be adjusted to obtain the WCF magnitude for either Case 1 or Case 2. In contrast, the maximum missed detection probability $p_{\mathrm{md,max}}$ can be obtained from the candidate searching interval $\mathscr{B}$ for Case 3. Specifically, if $p_{\mathrm{md,max}} > p_{\mathrm{md,exp}}$, the WCF magnitude corresponds to $p_{\mathrm{md,max}}$ in the candidate searching interval $\mathscr{B}$. Otherwise, the searching interval must also be adjusted to obtain the WCF magnitude for Case 3. In general, the searching interval is driven by the $p_{\mathrm{md,exp}}$ given the satellite geometry, the user range accuracy (URA) of observation and the faulty satellite. The improper $p_{\mathrm{md,exp}}$ will cause the absence of WCF magnitude within the searching interval, which could increase the calculation error of the MDPE. The valid searching interval is affected by the $p_{\mathrm{md,exp}}$. Therefore, it is necessary to analyse the impact of the $p_{\mathrm{md,exp}}$ on the searching interval.

3.2. Effect of expected missed detection probability

Two simulations will be carried out to analyse the effect of expected missed detection probability $p_{\mathrm{md,exp}}$. Firstly, numerical simulations are conducted to analyse the factors affecting the setting of $p_{\mathrm{md,exp}}$. Secondly, the impact of $p_{\mathrm{md,exp}}$ on the searching interval are examined. The single epoch geometry matrix for dual constellations is used for the numerical simulation,

$$\boldsymbol{G}_{\mathrm{BDS}} = \begin{bmatrix} 0\cdot4759 & -0\cdot5434 & 0\cdot6914 & 1 & 0 \\ -0\cdot1045 & -0\cdot9643 & 0\cdot2431 & 1 & 0 \\ 0\cdot7822 & 0\cdot3026 & 0\cdot5445 & 1 & 0 \\ -0\cdot8056 & 0\cdot1460 & 0\cdot5741 & 1 & 0 \\ -0\cdot1112 & 0\cdot6860 & 0\cdot7190 & 1 & 0 \\ -0\cdot3826 & -0\cdot6408 & 0\cdot6655 & 1 & 0 \\ -0\cdot8407 & 0\cdot3867 & 0\cdot3788 & 1 & 0 \\ 0\cdot7375 & 0\cdot5275 & 0\cdot4216 & 1 & 0 \\ 0\cdot2711 & -0\cdot9493 & 0\cdot1593 & 1 & 0 \end{bmatrix} \quad \boldsymbol{G}_{\mathrm{GPS}} = \begin{bmatrix} 0\cdot3086 & 0\cdot6870 & 0\cdot6578 & 0 & 1 \\ 0\cdot7837 & -0\cdot5887 & 0\cdot1977 & 0 & 1 \\ -0\cdot0908 & 0\cdot9269 & 0\cdot3641 & 0 & 1 \\ 0\cdot7090 & -0\cdot1221 & 0\cdot6945 & 0 & 1 \\ -0\cdot2546 & -0\cdot6945 & 0\cdot6729 & 0 & 1 \\ 0\cdot1904 & -0\cdot9447 & 0\cdot2669 & 0 & 1 \\ -0\cdot8137 & 0\cdot4985 & 0\cdot2988 & 0 & 1 \\ -0\cdot7261 & 0\cdot0690 & 0\cdot6840 & 0 & 1 \end{bmatrix}$$

The $\mathrm{P_{MD}}$ and $\mathrm{P_{FA}}$ were set as 10^{-3} and 10^{-5}, respectively. Furthermore, the satellite with the largest slope was chosen as the faulty satellite, and the AL was set to 35 m.

The candidate searching interval is invalid when the $p_{\mathrm{md,max}}$ is smaller than $p_{\mathrm{md,exp}}$. Since the $p_{\mathrm{md,exp}}$ is usually set as equal to the preset required $\mathrm{P_{MD}}$, the impact of different parameters on the $p_{\mathrm{md,max}}$ is investigated to attain the valid searching interval. It can be induced from Equation (2) that the URA, the number of satellites (NSat) and the AL can impact the $p_{\mathrm{md,max}}$. The AL is defined by RNP, which is not the focus in this contribution. Figure 1 shows the difference between $p_{\mathrm{md,max}}$ and $p_{\mathrm{md,exp}}$ with respect to the URA and the NSat. As seen in Figure 1, the difference between $p_{\mathrm{md,max}}$ and $p_{\mathrm{md,exp}}$ increases with either a smaller URA or more available satellites. The $p_{\mathrm{md,exp}}$ must be adjusted to reduce the difference between the $p_{\mathrm{md,exp}}$ and the $p_{\mathrm{md,max}}$ to acquire the valid searching interval.

The impact of $p_{\mathrm{md,exp}}$ on the searching interval construction is further analysed. The numerical simulation result is shown in Figure 2. The $p_{\mathrm{md,exp}}$ is set up as equal to the preset requirement $\mathrm{P_{MD}}$ as 10^{-3}. The green region in the figure indicates that the candidate searching interval is valid for the WCF magnitude searching. The grey region represents when the candidate searching interval cannot be

https://doi.org/10.1017/S0373463324000225 Published online by Cambridge University Press

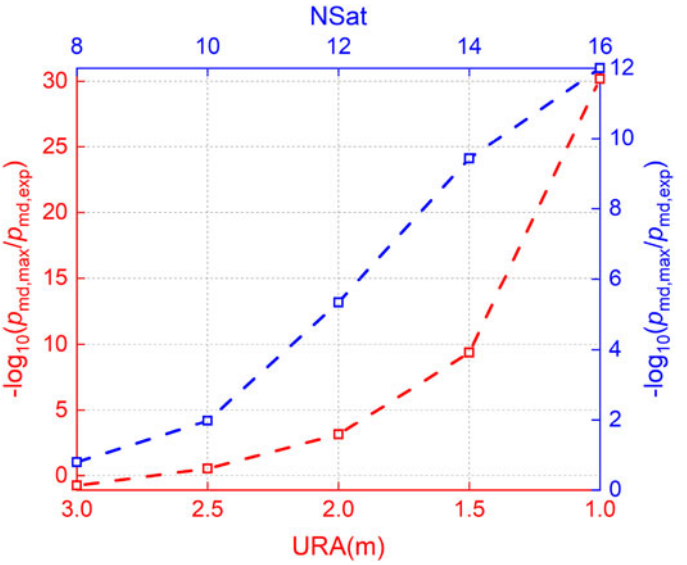

Figure 1. *Effect of the URA and NSat on the* $p_{\mathrm{md,max}}$ *and* $p_{\mathrm{md,exp}}$.

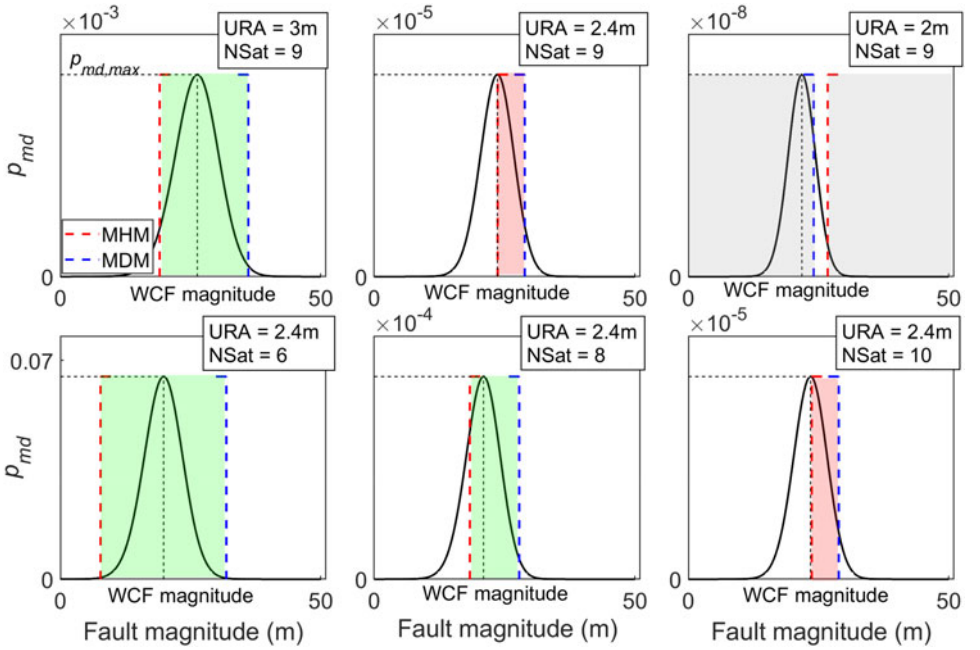

Figure 2. *Effect of the URA (top panel) and the NSat (bottom panel) on the searching interval construction.*

constructed because *MDM* is less than *MHM*. The red region shows the candidate searching interval can be constructed whilst the WCF magnitude is absent. As seen from Figure 2, a tighter searching interval is constructed with a smaller URA or more satellites, which may lead to the absence of WCF magnitude within the searching interval, as shown in the subpanels at the top-right, top-middle and bottom-right of the figure. Therefore, it is necessary to develop the searching interval adjustment by controlling $p_{\mathrm{md,exp}}$ to improve the WCF magnitude searching accuracy.

https://doi.org/10.1017/S0373463324000225 Published online by Cambridge University Press

3.3. Searching interval adjustment

From this analysis, it can be found that the valid searching interval must be adjusted until the $p_{md,exp}$ is consistent with $p_{md,max}$. Since the WCF magnitude has a higher likelihood to be contained within a loose searching interval, the $p_{md,exp}$ should be reduced firstly to introduce a loose searching interval. However, the computation burden will be unacceptable when an over loose searching interval is introduced by the over-small $p_{md,exp}$. The counterbalance between the efficiency and the accuracy of the WCF magnitude searching must be accounted for in the selection of $p_{md,exp}$.

For the implementation of the searching interval adjustment, the conditions that require searching interval adjustment must be identified. As induced from these three cases for searching intervals, we can summarise two conditions that initialise the searching interval adjustment. Firstly, *MDM* is smaller than *MHM*. Secondly, *MDM* is larger than *MHM* when the maximum calculated missed detection probability $p_{md,max}$ for the candidate searching interval is smaller than the $p_{md,exp}$. Either of these two conditions will initialise the searching interval adjustment.

The condition that terminates the searching interval adjustment and confirms the WCF magnitude must also be clarified. As the contrary to the conditions that initialise the searching interval adjustment, the searching interval adjustment is terminated when *MDM* is larger than *MHM* and the $p_{md,max}$ in the candidate searching interval exceeds the $p_{md,exp}$. These two constraints must be satisfied simultaneously to terminate the adjustment, in which the first constraint is to ensure that the searching interval can be constructed, and the second constraint is set to ensure the capture of WCF magnitude.

The flowchart of the proposed MDPE method is shown in Figure 3. The WCF magnitude is the key parameter for the rigorous MDPE and is determined through a two-step search. Specifically, the searching interval for the WCF magnitude is constructed by the combination of *MDM* and *MHM* in the first step. To avoid the absence of a WCF magnitude due to a potential over-tight searching interval, the searching interval adjustments are made in the second step by introducing the adjustment conditions of initialisation and termination, so that the counterbalance between the searching efficiency and the accuracy of the searching interval can be achieved. Through the WCF magnitude searching interval construction and adjustment, the missed detection probability of RAIM can be evaluated.

4. Experiment and analysis

To test the effectiveness of the proposed method in obtaining accurate WCF magnitudes and evaluating the missed detection probability performance, the simulation approach can be used to compare the proposed method and the traditional searching method without a searching interval adjustment. Firstly, the global WCF magnitude searching accuracy under different constellations and different URAs is analysed. Secondly, the MDPE among the classical RAIM methods under different WCF magnitude searching methods is carried out to verify the rigorousness of the proposed method.

The constellations of BDS and GPS were simulated to compute the WCF magnitude searching performance via an almanac file, in which the BDS constellation consisted of 29 satellites (2 GEO + 3 IGSO + 24 MEO) and the GPS constellation of 24 satellites. The simulation software is based on the MATLAB Algorithm Availability Simulation Tool (MAAST) provided by Stanford University. The mask angle was set up as 5 degrees. The satellite geometry was simulated every 10 min over the course of a day. The users were placed on a grid every 5 degrees in both latitude and longitude, for a total of 2,628 locations. Table 1 shows the parameters of the observation error model used in the simulation. The observation error model σ_i for each satellite is constructed as,

$$\sigma_i^2 = \sigma_{URA,i}^2 + \sigma_{trop,i}^2 + \sigma_{user,i}^2 \tag{12}$$

https://doi.org/10.1017/S0373463324000225 Published online by Cambridge University Press

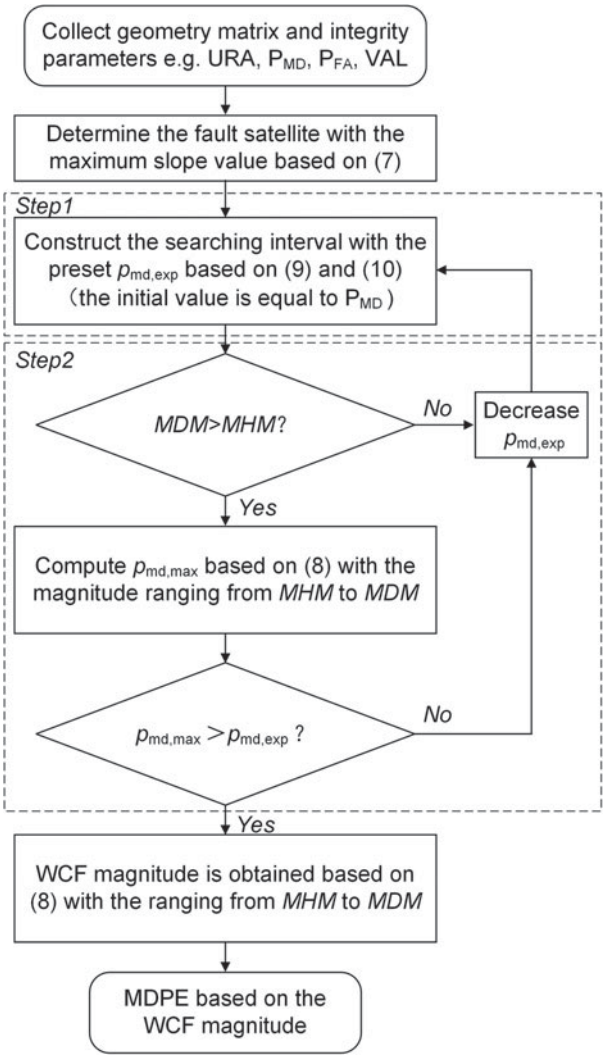

Figure 3. *Flowchart of the proposed MDPE implementation.*

Table 1. *Simulation parameters setting.*

Parameters	Value
P_{MD} requirement	10^{-3}
P_{FA} requirement	2×10^{-6}
Mask angle	5 deg
Time step	10 min
Simulation duration	24 h
WCF magnitude searching step	10^{-3} m
VAL	35 m
Residual tropospheric error (σ_{trop})	$0{\cdot}12[\mathrm{m}] \times 1{\cdot}001/(0{\cdot}002001 + \sin^2((\pi\theta)/180))^{1/2}$ (Blanch et al., 2015) (Blanch et al., 2015)
Smoothed code multipath (σ_{MP})	$0{\cdot}13[\mathrm{m}] + 0{\cdot}53[\mathrm{m}]\exp(-\theta/10[\mathrm{deg}])$ (Blanch et al., 2015)
Smoothed code receiver noise (σ_{Noise})	$0{\cdot}15[\mathrm{m}] + 0{\cdot}43[\mathrm{m}]\exp(-\theta/6{\cdot}9[\mathrm{deg}])$ (Blanch et al., 2015)

https://doi.org/10.1017/S0373463324000225 Published online by Cambridge University Press

The description of observation error model is given in Table 1, in which θ is the elevation in degree, $\sigma_{user,i}$ is the combination of the multipath and receiver noise as,

$$\sigma_{user,i} = \sqrt{\frac{f_1^4 + f_2^4}{\left(f_1^2 - f_2^2\right)^2}} \sqrt{\left(\sigma_{\mathrm{MP},i}\right)^2 + \left(\sigma_{\mathrm{Noise},i}\right)^2} \tag{13}$$

Note that the first-order ionospheric delay is assumed to be removed by the combination of dual-frequency observations.

4.1. WCF searching performance analysis

To sufficiently investigate the effect of satellite geometry on the accuracy of WCF magnitude searching, a global WCF magnitude error analysis for the proposed method was conducted. The WCF magnitude searching results were collected under the single BDS constellation and the BDS/GPS constellations, respectively. Moreover, we studied the WCF searching performance under the URA values of 2 m, 2·4 m, 3 m for both BDS and GPS (Zhao et al., 2021; Blanch et al., 2022). Figure 4 presents the simulation results. Two types of methods are compared, i.e. the WCF magnitude obtained from the proposed method with the searching interval adjustment, denoted as 'proposed method', and the searching method without searching interval adjustment, denoted as the 'no-adjustment method'. It should be noted that the reference of the WCF magnitude is obtained by the brute-forcing searching with a very loose searching interval without considering the cost of higher computation time. At each user location, the 95th percentile searching error of WCF magnitude was selected to illustrate the accuracy of WCF magnitude searching. The searching error is defined as the difference between the WCF magnitude obtained from the candidate method and the reference.

Figure 4 shows the global WCF magnitude searching error for different simulation cases. It can be found that the global WCF magnitude searching error of the no-adjustment method increases with either a smaller URA or more satellites. Furthermore, the WCF magnitude searching error based on the no-adjustment method in the Asia Pacific Region is larger than other locations. This is because that the tighter searching interval will be obtained by the no-adjustment method with a smaller URA or more available satellites, which may induce the absence of the WCF magnitude within the searching interval. In contrast, the proposed method offers a remarkable reduction of the global WCF magnitude searching error, regardless of the grade of URA and the number of satellites. This is because the tightness of the WCF magnitude searching interval can be adjusted by the proposed method. The difference between the proposed method and the no-adjustment method demonstrates the superior performance of the proposed method in reducing the worldwide WCF magnitude searching error. We further analyse the impact of the WCF magnitude searching error on the MDPE error based on Equation (2). Note that the MDPE error is defined as the difference between the maximum of the evaluated missed detection probability from the searching interval and the reference.

The impacts of the WCF magnitude searching error on the MDPE error are shown by Figures 5 and 6. The MDPE error increases with either a decrease of URA or an increase in the number of satellites, which is consistent with the results of the WCF magnitude searching error. In the extreme case, the MDPE can be more than 10^{-3} level by the no-adjustment method. It should be note that the MDPE error with a 10^{-3} level is unacceptable because the error is much larger than the preset missed detection probability requirement P_{MD}. In contrast, the MDPE by the proposed method is less than the no-adjustment method. The worst MDPE from the proposed method can be maintained at 10^{-7} level, which is much smaller than the preset missed detection probability requirement. The better MDPE performance can be attributed as searching interval adjustment. The simulations results show that the higher accuracy of both the WCF magnitude searching and the MDPE can be obtained by the proposed interval adjustment method.

https://doi.org/10.1017/S0373463324000225 Published online by Cambridge University Press

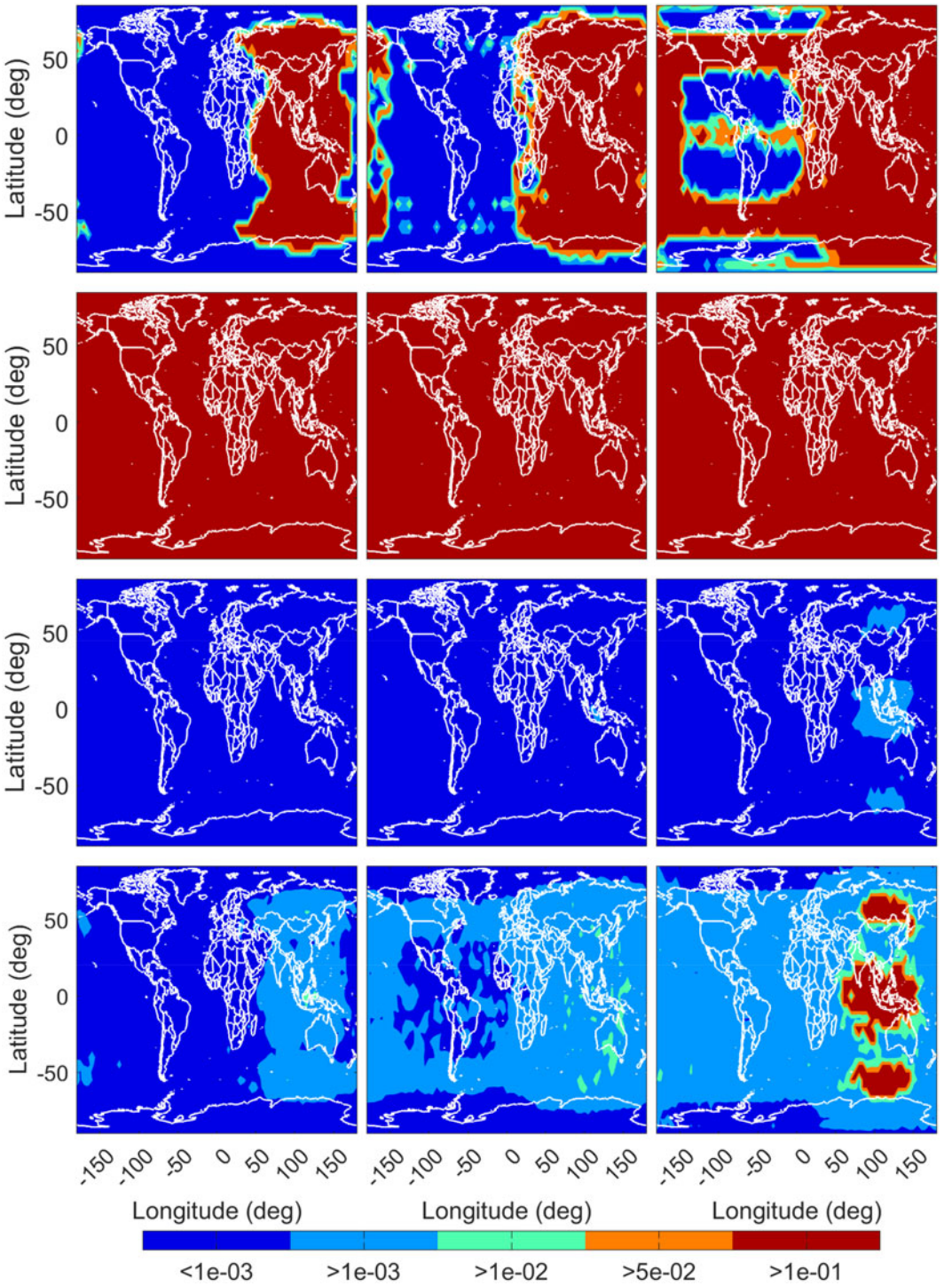

Figure 4. *Searching error of the WCF magnitude (m). The column panels from left to right represent the URA of 3 m, 2·4 m and 2 m, respectively. The row panels from top to bottom represent the traditional method with no adjustment for BDS, the traditional method for BDS/GPS, the proposed method with searching interval adjustment for BDS, and the proposed method for BDS/GPS, respectively.*

https://doi.org/10.1017/S0373463324000225 Published online by Cambridge University Press

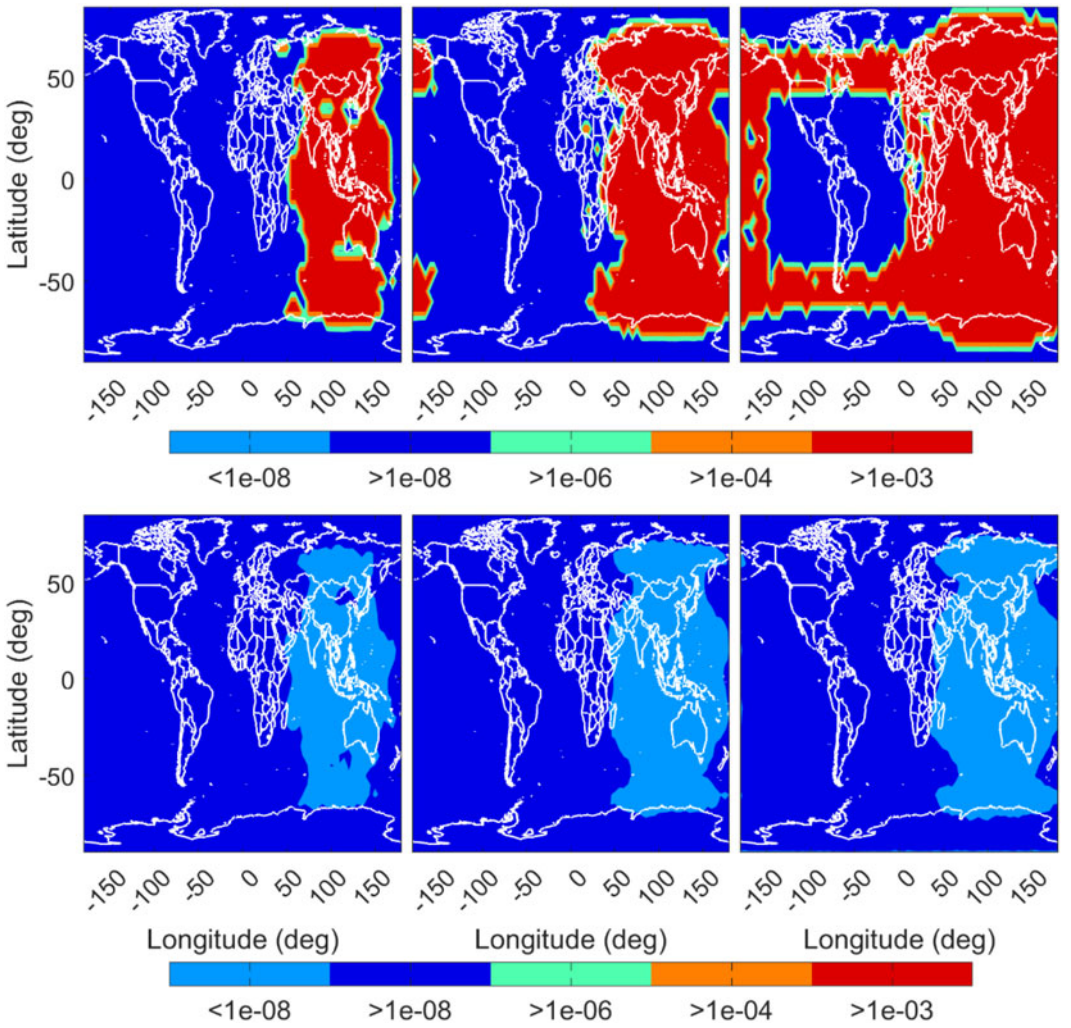

Figure 5. *Missed detection probability evaluation error under BDS constellation. The columns from left to right represent different URA of 3 m, 2·4 m and 2 m, respectively. The row panels from top to bottom represent the traditional method with no adjustment and the proposed method with searching interval adjustment, respectively.*

4.2. Simulation experiment result

The MDPE process is carried out using different RAIM algorithms. Specifically, the fault magnitude determination methods are the proposed method with searching interval adjustment and the traditional method with no adjustment. The RAIM algorithms are three types of PL computation methods: the classic PL computation method can be seen from Milner and Ochieng (2011), denoted as 'PL_{BC}'; the PL computation method proposed by Walter and Enge (1995), denoted as 'PL_{WE}'; and the method proposed by Brown and Chin (1998), denoted as 'PL_{BC+}'. We strictly follow the integrity monitoring evaluation process outlined in RTCA DO-229A (2006) to inject the WCF magnitude into the observation of the WCF satellite. To evaluate the probability, the Monte Carlo iterations of 10^4 for an epoch is tried, and the evaluated missed detection probability was compared with the predefined P_{MD} to verify if the missed detection probability of the RAIM algorithm was satisfied. A total of $3{\cdot}7843 \times 10^9$ space-time samples were generated across all the satellite geometry. Note that the *a posteriori* missed detection

https://doi.org/10.1017/S0373463324000225 Published online by Cambridge University Press

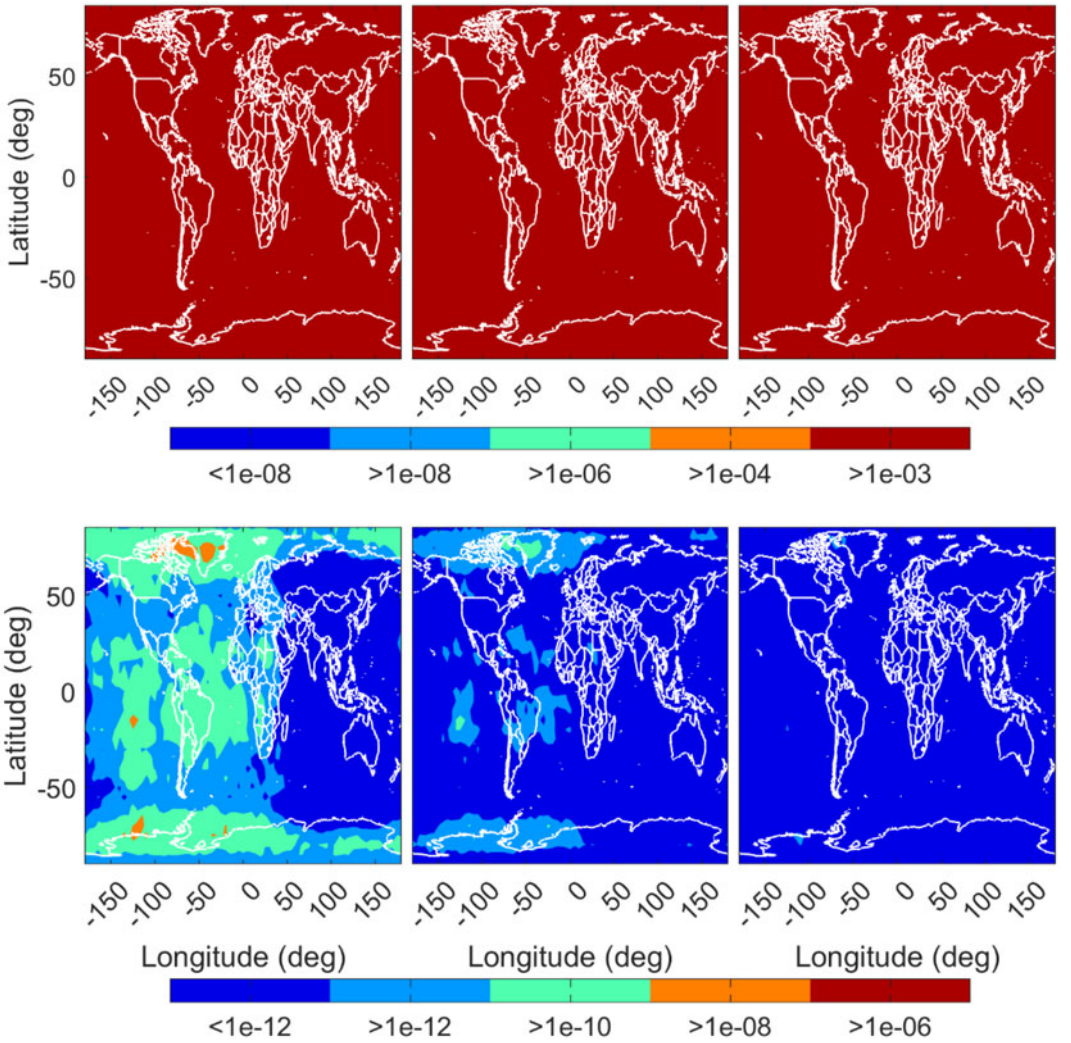

Figure 6. *Missed detection probability evaluation error with BDS/GPS constellation. The columns from left to right represent the URA values of 3 m, 2·4 m and 2 m, respectively. The row panels from top to bottom represent the traditional method with no adjustment and the proposed method with searching interval adjustment, respectively.*

case is verified when the PE is more than the PL, whilst the test statistic is less than the detection threshold (RTCA DO-229A, 2006; Li et al., 2016). The missed detection probability performance among these three RAIM algorithms was compared with the metric of missed detection rate to verify the rigorousness of the proposed method in obtaining maximum missed detection probability, in which the missed detection rate is defined as the ratio between the epochs of missed detection and the total number of epochs. The reference of missed detection rate was obtained from the *a posteriori* missed detection rate by injecting the WCF magnitude resulting from a loose empirical searching interval.

To demonstrate the rigorousness of the proposed method, the averaged missed detection rate all over the world is computed for different constellations, and URAs are shown in Table 2. It is observed that the missed detection rate evaluated by the proposed method is closest to the reference of missed detection rate, regardless of the types of RAIM algorithm, which demonstrates the rigorousness of the proposed MDPE method. Furthermore, when compared with the reference, the missed detection rate

https://doi.org/10.1017/S0373463324000225 Published online by Cambridge University Press

Table 2. *Comparison of missed detection rates from different RAIM algorithms.*

Simulation parameters	WCF searching method	Missed detection rate		
		PL_{BC}	PL_{WE}	PL_{BC+}
BDSURA = 3 m	No adjustment	$8{\cdot}050\times10^{-3}$	$1{\cdot}262\times10^{-4}$	$4{\cdot}817\times10^{-7}$
	Proposed	$8{\cdot}050\times10^{-3}$	$1{\cdot}265\times10^{-4}$	$6{\cdot}699\times10^{-7}$
	Reference	$8{\cdot}050\times10^{-3}$	$1{\cdot}265\times10^{-4}$	$6{\cdot}699\times10^{-7}$
BDSURA = 2·4 m	No adjustment	$7{\cdot}799\times10^{-3}$	$1{\cdot}373\times10^{-3}$	$4{\cdot}816\times10^{-7}$
	Proposed	$7{\cdot}799\times10^{-3}$	$1{\cdot}373\times10^{-3}$	$6{\cdot}802\times10^{-7}$
	Reference	$7{\cdot}799\times10^{-3}$	$1{\cdot}373\times10^{-3}$	$6{\cdot}802\times10^{-7}$
BDSURA = 2 m	No adjustment	$7{\cdot}533\times10^{-4}$	$1{\cdot}495\times10^{-3}$	$4{\cdot}817\times10^{-7}$
	Proposed	$7{\cdot}533\times10^{-4}$	$1{\cdot}495\times10^{-3}$	$6{\cdot}935\times10^{-7}$
	Reference	$7{\cdot}533\times10^{-4}$	$1{\cdot}495\times10^{-3}$	$6{\cdot}935\times10^{-7}$
BDS/GPSURA = 3 m	No adjustment	$2{\cdot}315\times10^{-2}$	$1{\cdot}302\times10^{-4}$	$5{\cdot}021\times10^{-7}$
	Proposed	$2{\cdot}315\times10^{-2}$	$1{\cdot}304\times10^{-4}$	$1{\cdot}186\times10^{-6}$
	Reference	$2{\cdot}315\times10^{-2}$	$1{\cdot}304\times10^{-4}$	$1{\cdot}186\times10^{-6}$
BDS/GPSURA = 2·4 m	No adjustment	$2{\cdot}259\times10^{-2}$	$1{\cdot}325\times10^{-4}$	$5{\cdot}022\times10^{-7}$
	Proposed	$2{\cdot}259\times10^{-2}$	$1{\cdot}325\times10^{-4}$	$1{\cdot}161\times10^{-6}$
	Reference	$2{\cdot}259\times10^{-2}$	$1{\cdot}325\times10^{-4}$	$1{\cdot}161\times10^{-6}$
BDS/GPSURA = 2 m	No adjustment	$2{\cdot}205\times10^{-2}$	$1{\cdot}345\times10^{-4}$	$5{\cdot}022\times10^{-7}$
	Proposed	$2{\cdot}205\times10^{-2}$	$1{\cdot}347\times10^{-4}$	$1{\cdot}137\times10^{-6}$
	Reference	$2{\cdot}205\times10^{-2}$	$1{\cdot}347\times10^{-4}$	$1{\cdot}137\times10^{-6}$

of PL_{BC} and PL_{WE} methods is much higher than with the PL_{BC+} method. As shown in Figures 4–6, although the WCF searching accuracy of the proposed method is higher than the traditional method, the reduction of missed detection rate error with a higher WCF searching accuracy can be disregarded when the missed detection rate of RAIM is higher than 10^{-4}. Correspondingly, the benefit of higher WCF searching accuracy can be more for the RAIM with a much lower missed detection rate. Therefore, it can be seen that the missed detection rate of the proposed method is comparable with the traditional method for the RAIM with a higher missed detection rate. In contrast, the proposed method shows better MDPE performance than the traditional method for the RAIM algorithms, with a lower missed detection rate at the order of either 10^{-7} or 10^{-6}. In addition, the proposed method can improve the accuracy of the evaluated missed detection rate by at most 57·66% relative to the no-adjustment method among the different classical RAIM algorithms, which illustrates the higher accuracy of WCF magnitude searching. The proposed method can improve the accuracy of the evaluated missed detection rate by at most 29·57% compared with the no-adjustment method when dual-constellations are introduced. Moreover, the PL_{WE} and PL_{BC+} method can satisfy the requirement P_{MD} regardless of the grade of URA and the constellation configuration, and the PL_{BC+} method can provide much better missed detection rate performance than the other two RAIM algorithms because the PL of the PL_{BC+} method is the most conservative of these three RAIM algorithms. The test result is consistent with the research findings in Angus (2007) and Milner and Ochieng (2011).

4.3. Positioning experiment result

We conducted a positioning experiment to further analyse the MDPE performance of the proposed method utilising real-world data. The raw observation data came from the IGS and the time span of data collection was five days with a sampling interval of 30 s. Four stations, i.e. JFNG, TLSG, GODS and ZAMB, were selected for the experiment. The WCF obtained from the traditional no-adjustment

https://doi.org/10.1017/S0373463324000225 Published online by Cambridge University Press

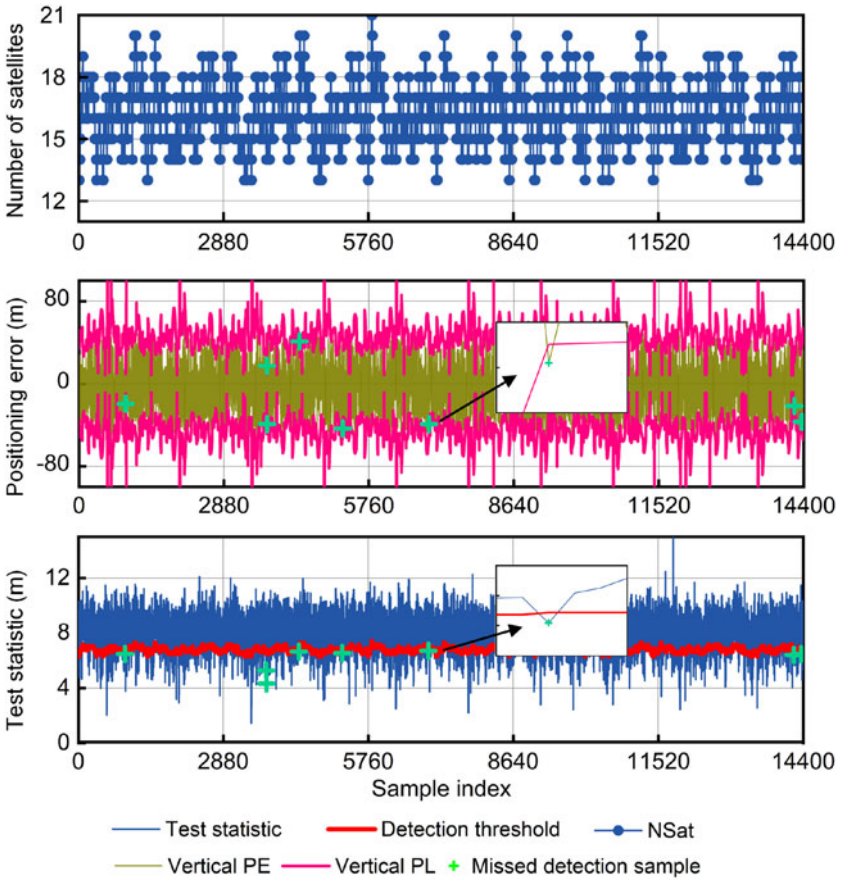

Figure 7. *Positioning error and test statistics in JFNG. The green crosses in the panels indicate the missed detection samples.*

method and the proposed method was injected to the raw observation to verify the performance of the typical RAIM algorithms introduced at the previous section. The epoch that the test statistic is lower than the detection threshold and the PE exceeds the PL is flagged as the missed detection sample.

The positioning result and the fault detection result of JFNG is shown in Figure 7. Note that the test statistics and the detection threshold can be reference from Section 2. The PL is computed based on the PL_{WE} method. It can be seen from Figure 7 that lots of the positioning errors exceed the corresponding PL because of the injected WCF. Furthermore, a few missed detection samples can be observed. Most of the missed detection samples are present when the number of satellites is small because the fault detection power of RAIM is undermined by the decreased observation redundancy. The missed detection rate results based on the positioning experiments of different RAIM algorithms are listed in Table 3. The table indicates that the MDPE of the traditional method is optimistic for different RAIM algorithms regardless of location. In contrast, the proposed method is closer to the reference than the traditional method for different RAIM algorithms, which proves the effectiveness of the proposed method in MDPE.

5. Conclusions

To evaluate the performance of RAIM algorithms in the presence of a fault, a MDPE method is proposed to evaluate the maximum missed detection probability based on the WCF magnitude searching. The WCF magnitude searching interval is constructed by the combination of *MDM* and *MHM*. Based on the

https://doi.org/10.1017/S0373463324000225 Published online by Cambridge University Press

Table 3. *Missed detection rate results of positioning experiment.*

Station	WCF searching method	Missed detection rate		
		PL_{BC}	PL_{WE}	PL_{BC+}
JFNG	No adjustment	$3{\cdot}5\times10^{-3}$	$6{\cdot}25\times10^{-4}$	$1{\cdot}39\times10^{-4}$
	Proposed	$3{\cdot}7\times10^{-3}$	$6{\cdot}94\times10^{-4}$	$2{\cdot}08\times10^{-4}$
	Reference	$3{\cdot}7\times10^{-3}$	$6{\cdot}94\times10^{-4}$	$2{\cdot}08\times10^{-4}$
TLSG	No adjustment	$1{\cdot}9\times10^{-3}$	$4{\cdot}86\times10^{-4}$	$1{\cdot}39\times10^{-4}$
	Proposed	$2{\cdot}0\times10^{-3}$	$4{\cdot}86\times10^{-4}$	$2{\cdot}08\times10^{-4}$
	Reference	$2{\cdot}0\times10^{-3}$	$4{\cdot}86\times10^{-4}$	$2{\cdot}08\times10^{-4}$
GODS	No adjustment	$1{\cdot}7\times10^{-3}$	$3{\cdot}47\times10^{-4}$	$6{\cdot}94\times10^{-5}$
	Proposed	$1{\cdot}8\times10^{-3}$	$4{\cdot}86\times10^{-4}$	$2{\cdot}08\times10^{-4}$
	Reference	$1{\cdot}8\times10^{-3}$	$4{\cdot}86\times10^{-4}$	$2{\cdot}08\times10^{-4}$
ZAMB	No adjustment	$2{\cdot}2\times10^{-3}$	$2{\cdot}08\times10^{-4}$	0·00
	Proposed	$2{\cdot}3\times10^{-3}$	$2{\cdot}78\times10^{-4}$	$6{\cdot}94\times10^{-5}$
	Reference	$2{\cdot}3\times10^{-3}$	$2{\cdot}78\times10^{-4}$	$6{\cdot}94\times10^{-5}$

sensitivity simulation of the expected missed detection probability with respect to the WCF magnitude searching accuracy, it has been revealed that the expected missed detection probability impacted by the URA and the number of satellites must be adjusted to contain the WCF magnitude within the searching interval. To address this issue, the searching interval adjustment is designed to avoid the absence of the WCF magnitude.

The simulation result has demonstrated that the proposed searching interval adjustment method can obtain the accurate WCF magnitude. Furthermore, the accuracy of worldwide evaluated missed detection rate can achieve an improvement of 57·66% at most by the proposed method for the different classical RAIM algorithms, which demonstrates that a rigorous MDPE can be achieved. The accuracy of evaluated missed detection rate can be further improved when the dual-constellations are introduced. Additionally, a positioning experiment further verifies that the proposed method can achieve stricter MDPE than the traditional method. It is noted that the single-satellite fault is considered in this contribution, which is constrained by the construction of searching interval for the multiple-faults. Future work will extend to the multiple-faults hypotheses.

Acknowledgement. This research was jointly funded by the National Key Research and Development Program (No. 2021YFB3901300), the National Natural Science Foundation of China (Nos. 62373117, 62403158).

Competing Interests. The authors declare none.

References

Angus, J. E. (2007). RAIM with multiple faults. *Navigation*, **53**(4), 249–257.

Blanch, J. and Walter, T. (2020). Stressing Testing Advanced RAIM Airborne Algorithms. *Proceedings of the 2020 International Technical Meeting of The Institute of Navigation*, San Diego, California, 421–439.

Blanch, J., Walter, T., Enge, P., Lee, Y., Pervan, B., Rippl, M., Spletter, A. and Kropp, V. (2015). Baseline advanced RAIM user algorithm and possible improvements. *IEEE Transactions on Aerospace and Electronic Systems*, **51**(1), 713–732.

Blanch, J., Walter, T., Milner, C., Joerger, M., Pervan, B. and Bouvet, D. (2022). Baseline Advanced RAIM User Algorithm: Proposed Updates. *Proceedings of the 2022 International Technical Meeting of The Institute of Navigation*, Long Beach, California, 229–251.

Brown, R. G. and Chin, G. Y. (1998). *Calculation of threshold and protection radius using chi-square methods-a geometric approach*. ION Red Books.

Jiang, Y. and Wang, J. (2014). A new approach to calculate the vertical protection level in a-RAIM. *Journal of Navigation*, **67**(4), 711–725.

Joerger, M., Chan, F. C. and Pervan, B. (2014). Solution separation versus residual-based RAIM. *Navigation*, **61**(4), 273–291.

https://doi.org/10.1017/S0373463324000225 Published online by Cambridge University Press

Kaleta, W. Z. and Skorupski, J. (2019). A fuzzy inference approach to analysis of LPV-200 procedures influence on air traffic safety. *Transportation Research Part C: Emerging Technologies*, **106**(4), 264–280.
Lee, Y., Bian, B., Odeh, A. and She, J. (2021). Sensitivity of advanced RAIM performance to mischaracterizations in integrity support message values. *Navigation*, **68**(3), 541–558.
Li, L., Quddus, M., Ison, S. and Zhao, L. (2012). Multiple reference consistency check for LAAS: A novel position domain approach. *GPS Solutions*, **16**(2), 209–220.
Li, L., Li, Z., Yuan, H., Wang, L. and Hou, Y. (2016). Integrity monitoring based ratio test for GNSS integer ambiguity validation. *GPS Solutions*, **20**(3), 573–585.
Li, L., Wang, H., Jia, C., Zhao, L. and Zhao, Y. (2017). Integrity and continuity allocation for the RAIM with multiple constellations. *GPS Solutions*, **21**(4), 1503–1513.
Milner, C. and Ochieng, W. (2009). A fast and efficient integrity computation for non-precision approach performance assessment. *GPS Solutions*, **14**(2), 193–205.
Milner, C. and Ochieng, W. (2011). Weighted RAIM for APV: The ideal protection level. *Journal of Navigation*, **64**(1), 61–73.
Milner, C., Pervan, B., Blanch, J. and Joerger, M. (2020). Evaluating Integrity and Continuity Over Time in Advanced RAIM. *Proceedings of IEEE/ION PLANS 2020*, Portland, Oregon, 502–514.
Ober, P. B. (2003). Integrity prediction and monitoring of navigation systems. Ph.D. thesis. TU Delft.
RTCA DO-229D (2006). Minimum operational performance standards for GPS/WAAS airborne equipment.
Walter, T. and Enge, P. (1995). Weighted RAIM for Precision Approach. *Proceedings of the 1995 International Technical Meeting of the Institute of Navigation*, Palm Springs, Palm Springs, 1995–2004.
Wang, L., Li, L., Li, R., Li, M. and Cheng, L. (2023). Worst-case integrity risk sensitivity for RAIM with constellation modernization. *Remote Sensing*, **15**(12), 2979–2994.
Zhai, Y., Zhan, X. and Pervan, B. (2020). Bounding integrity risk and false alert probability over exposure time intervals. *IEEE Transactions on Aerospace and Electronic Systems*, **56**(3), 1873–1885.
Zhao, P., Joerger, M., Liang, X., Pervan, B. and Liu, Y. (2020). A new method to bound the integrity risk for residual-based ARAIM. *IEEE Transactions on Aerospace and Electronic Systems*, **57**(2), 1378–1383.
Zhao, Y., Cheng, C., Li, L. and Wang, R. (2021). BDS signal-in-space anomaly probability analysis over the last 6 years. *GPS Solutions*, **25**(49), 25–49.
Zhu, C., Meurer, M. and Joerger, M. (2023). Integrity Analysis for Greedy Search Based Fault Exclusion with A Large Number of Faults. In: *IEEE/ION Position, Location and Navigation Symposium (PLANS)*, 430–435.

Appendix A: The missed detection probability analysis for Case 1

This section aims to prove that the missed detection probability for any fault magnitude is smaller than the expected missed detection $p_{\mathrm{md,exp}}$ when $MDM \le MHM$.

Firstly, the missed detection probability based on Equation (2) can be bounded as,

$$p_{\mathrm{md}} = P\{|\varepsilon| > l|H_i\} \times P\{q < T|H_i\} \le P\{|\varepsilon| > l^*|H_i\} \times P\{q < T|H_i\} \tag{A1}$$

where l^* is smaller than the specified alarm limit l.

When $MDM \le MHM$, we have $l \ge cd + K_{\mathrm{md,exp}}\sigma$, where,

$$\begin{cases} c = \dfrac{\lambda_{\mathrm{md,exp}}}{||\boldsymbol{M}\bar{\boldsymbol{F}}||} \\ d = |\boldsymbol{h}^{*\mathrm{T}}\bar{\boldsymbol{F}}| \end{cases} \tag{A2}$$

we can substitute $l^* = cd + K_{\mathrm{md,exp}}\sigma$ and Equations (3) and (4) into Equation (A1),

$$\begin{aligned} p_{\mathrm{md}} &\le \left(\Phi\left[\frac{l^* + \boldsymbol{h}^{*\mathrm{T}}\bar{\boldsymbol{F}}b}{\sigma}\right] + \Phi\left[\frac{l^* - \boldsymbol{h}^{*\mathrm{T}}\bar{\boldsymbol{F}}b}{\sigma}\right]\right)\chi^2_{T,n-m}[\lambda^2] \\ &\le 2\Phi\left[\frac{l^* - |\boldsymbol{h}^{*\mathrm{T}}\bar{\boldsymbol{F}}|b}{\sigma}\right]\chi^2_{T,n-m}[\lambda^2] \\ &\le 2\Phi\left[\frac{d(c-b)}{\sigma} + K_{\mathrm{md,exp}}\right]\chi^2_{T,n-m}[\lambda^2] \end{aligned} \tag{A3}$$

https://doi.org/10.1017/S0373463324000225 Published online by Cambridge University Press

When $c-b \geq 0$, we can have

$$\begin{aligned} p_{\text{md}} &\leq 2\Phi\left[\frac{d(c-b)}{\sigma} + K_{\text{md,exp}}\right] \chi^2_{T,n-m}[\lambda^2] \\ &\leq 2\Phi[K_{\text{md,exp}}] = p_{\text{md,exp}} \end{aligned} \tag{A4}$$

When $c-b < 0$, then, the expected missed detection $p_{\text{md,exp}}$ can bound the probability of detection failure because the actual noncentrality parameter $\lambda = ||\boldsymbol{M}\bar{\boldsymbol{F}}||b > \lambda_{\text{md,exp}}$ (Angus, 2007),

$$\begin{aligned} p_{\text{md}} &\leq 2\Phi\left[\frac{d(c-b)}{\sigma} + K_{\text{md,exp}}\right] \chi^2_{T,n-m}[\lambda^2] \\ &\leq \chi^2_{T,n-m}[\lambda^2] \\ &\leq \chi^2_{T,n-m}[\lambda^2_{\text{md,exp}}] = p_{\text{md,exp}} \end{aligned} \tag{A5}$$

From the combination of Equations (A4) and (A5), we demonstrate the missed detection probability for any fault magnitudes is smaller than the expected missed detection $p_{\text{md,exp}}$ when $MDM \leq MHM$.

Appendix B: The missed detection probability analysis for Case 2

We will prove the missed detection probability based on Equation (10) for the fault magnitudes within the candidate searching interval $\mathscr{B}$ is smaller than the expected missed detection probability $p_{\text{md,exp}}$ when $MHM < MDM$ and $\mathscr{B} \in (0, MHM) \cup (MDM, \infty)$.

When $0 < b < MHM$, the missed detection probability based on Equation (2) can be bounded as,

$$p_{\text{md}} = P(|\varepsilon| > l|H_i) \times P(q < T|H_i) \leq P(|\varepsilon| > l|H_i) \tag{B1}$$

Because the probability of positioning failure increases with a larger b (Milner and Ochieng, 2011), we can have,

$$\begin{aligned} P(|\varepsilon| > l|H_i) &\leq 2\Phi\left[\frac{l - |\boldsymbol{h}^{*\text{T}}\bar{\boldsymbol{F}}|b}{\sigma}\right] \\ &\leq 2\Phi\left[\frac{l - |\boldsymbol{h}^{*\text{T}}\bar{\boldsymbol{F}}|MHM}{\sigma}\right] = p_{\text{md,exp}} \end{aligned} \tag{B2}$$

Therefore,

$$p_{\text{md}} = P(|\varepsilon| > l|H_i) \times P(q < T|H_i) \leq P(|\varepsilon| > l|H_i) \leq p_{\text{md,exp}} \tag{B3}$$

For $b > MDM$, the missed detection probability based on (2) also can be bounded as,

$$p_{\text{md}} = P(|\varepsilon| > l|H_i) \times P(q < T|H_i) \leq P(q < T|H_i) \tag{B4}$$

When a noncentrality parameter λ is larger than $\lambda_{\text{md,exp}}$, the expected missed detection $p_{\text{md,exp}}$ can bound the probability of detection failure (Angus, 2007),

$$\begin{aligned} P(q < T|H_i) &= \chi^2_{T,n-m}[\lambda^2 = ||\boldsymbol{M}\bar{\boldsymbol{F}}b||^2] \\ &\leq \chi^2_{T,n-m}[\lambda^2_{\text{md,exp}} = ||\boldsymbol{M}\bar{\boldsymbol{F}}MDM||^2] = p_{\text{md,exp}} \end{aligned} \tag{B5}$$

https://doi.org/10.1017/S0373463324000225 Published online by Cambridge University Press

Therefore,

$$p_{\mathrm{md}} = P(|\varepsilon| > l|H_i) \times P(q < T|H_i) \leq P(q < T|H_i) \leq p_{\mathrm{md,exp}} \tag{B6}$$

From the combination of Equations (B3) and (B6), we demonstrate the missed detection probability for any fault magnitudes is smaller than the expected missed detection $p_{\mathrm{md,exp}}$ when $MHM < MDM$ and $\mathscr{B} \in (0, MHM) \cup (MDM, \infty)$.

Cite this article: Li R, Li L, Wang L, Li M, Na Z (2024). Missed detection probability evaluation for the RAIM based on worst-case fault magnitude searching. *The Journal of Navigation* 1–18. https://doi.org/10.1017/S0373463324000225